Ion Acoustic Waves in a Density Gradient

N. D'Angelo

Danish Space Research Institute, Lyngby, Denmark, and Research Establishment Risø, Roskilde, Denmark

and P. Michelsen and H. L. Pécseli

Association Euratom-AEK, Danish Atomic Energy Commission
Research Establishment Risø, Roskilde, Denmark

(Z. Naturforsch. **31 a**, 578–582 [1976]; received March 9, 1976)

A damping-growth transition for ion acoustic waves propagating in a non-uniform plasma (*e*-folding lengths for the density l_n) is observed at wavelengths $\lambda_c \approx 2\pi l_n$. The experiment, conducted in a *Q*-device, supports calculations performed in connection with the problem of solar corona heating.

I. Introduction

The propagation of ion acoustic waves in density gradients is of interest for plasmas in a gravitational field. Theoretical work based on a Vlasov model with special reference to the solar corona was performed by Parkinson and Schindler [1]. Liu [2] included also the effect of a magnetic field. A result of these investigations is the prediction of a (Landau) damping of the waves for wavelengths, λ, small compared to the *e*-folding length, l_n, of the density gradient while a growth in relative amplitude, $\tilde{n}/n_0$, is predicted for λ's much larger than l_n. The critical wavelength for the case where $T_i = T_e$ is $\lambda_c = 2\pi l_n$.

For high electron-to-ion temperature ratios, T_e/T_i, a fluid model is appropriate. In an experiment performed in a "diffusion plasma" with an imposed density gradient, Doucet et al.[3] found good agreement between experimental results and a simplified fluid picture for waves traveling from low density regions into regions of higher density.

In this paper we describe an experiment performed in the cesium plasma column of a conventional single ended Q-machine [4] in which $T_i \approx T_e$. In our case Landau damping of ion acoustic waves is an important process and the transition from damping to relative growth can be investigated. Although our plasma conditions are different from those considered by Parkinson and Schindler [1] and by Liu [2], our measurements reveal essentially the same features as resulted from their calculations.

Reprints requests to P. Michelsen, Danish Atomic Energy Commission, Research Establishment Risø, *4000-Roskilde*, Denmark.

Preliminary results from our measurements are published in Reference [5]. The present paper, in addition to much more detailed results on wave measurements, contains a description of the zero order state.

II. Experimental Set-Up

The experiment was performed in a cesium plasma produced by surface ionization in a conventional single ended *Q*-machine [4]. The plasma column is ~ 3 cm in diameter and confined by a homogeneous $\boldsymbol{B}$ field of intensity ~ 2500 Gauss. Plasma densities are $1-5\times10^9$ cm^{-3}, with temperatures $T_i \approx T_e \approx 2200$ °K. The neutral pressure is $\lesssim 10^{-5}$ mm Hg. Collisions are thus unimportant for the propagation of density perturbations. A (variable) density gradient along the direction of the $\boldsymbol{B}$ field is produced by surrounding a portion of the plasma column with a brass tube of length 15 cm and 3.5 cm inner diameter, biased to -30 volt to -100 volt with respect to the generating plate of the Q-device. This set-up is similar to the one described in Reference [6]. Ion acoustic waves are excited, in much the same manner as e.g. in Wong et al. [7], by a thin nickel mesh with ~ 140 0.8×0.8 mm^2 holes per cm^2 immersed in the plasma (normal to the axis of the column) between the hot plate and the brass tube. The plasma is terminated by a plate negatively biased in order to reflect all the electrons.

The steepness of the axial density profile (density decreasing from grid to tube) can be varied by varying the negative tube bias, more negative voltages on the tube giving rise to steeper density profiles. The tube has two effects on the plasma. First there is a lowering of the plasma potential, which causes an acceleration of the ions. The tube also gives rise to radial plasma losses by "scrape off" of ions (the Larmor radius being ~ 0.5 cm) or by ex-

citation of an instability which causes enhanced radial diffusion (for inst. a gravitational instability generated by the $\boldsymbol{E}\times\boldsymbol{B}$ rotation [8]). The resulting density gradient depends (apart from the tube voltage) on the magnetic field strength, lower B's giving rise to steeper profiles.

Measurements have been performed by means of a Langmuir probe, movable over a distance of ~ 25 cm along the axis of the plasma column, the exposed surface of the probe being a flat metal disc, 0.5 cm in diameter, oriented normal to the column axis. The zero order axial density profile is obtained most easily through a measurement of the probe floating potential and the relation [4, 7]

$$\varkappa T_e \,\partial n_0/\partial x = e\, n_0\, \partial \Phi_0/\partial x \qquad (1)$$

between density and potential gradients (we consider the electrons as isothermal i.e. T_e = const). Figure 1a shows the measured potential profile for

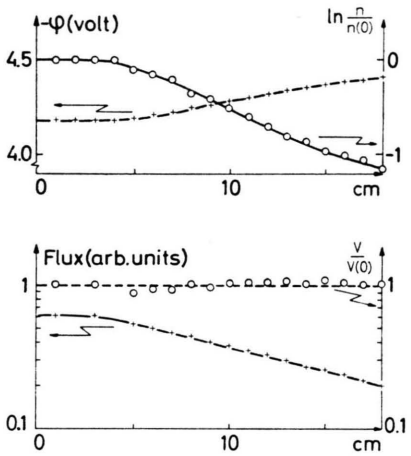

Fig. 1. a) Floating potential and density distribution along the column axis ($V_{tube} = -30$ V, $B = 2000$ gauss). b) Flux and axial velocity distribution for the same conditions of Figure 1 a.

one tube potential. Measurements of the total ion flux, nV, to the probe serve to determine the radial losses, $\mu_0(x)$, since

$$\frac{\partial (n_0 V_0)}{\partial x} = -\mu_0(x) \qquad (2)$$

in steady state conditions. Figures 1a and 1b show that $\mu_0(x) \cong n_0 \gamma$ where γ = constant, with good approximation. Finally we can determine the drift velocity $V_0(x)$ since we know the flux and density variation along the column axis (see Figure 1b). No large relative variation of $V_0(x)$ is expected with increasing x, since $V_0(x_0)$ is already larger than C_s (the sound speed) because of the sheath drop at the generating plate.

III. Wave Measurements

The wave measurements were performed using the Langmuir probe described in Section II. Only the relative fluctuations are of interest; thus all measurements were performed with the probe electrically floating since $\tilde{n}/n_0 \simeq e\,\tilde{\Phi}/\varkappa T_e$ ($\tilde{n}$ is the perturbed density, $\tilde{\Phi}$ the perturbed potential). The results of the wave measurements are summarized in Figure 2. During these measurements the bias of

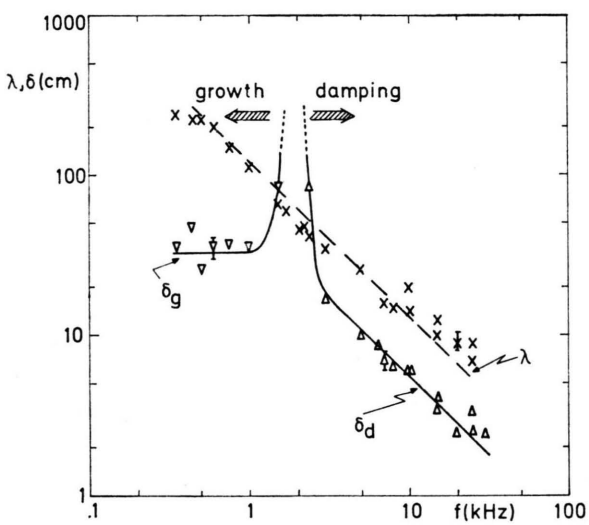

Fig. 2. The wavelength, λ, and the damping, δ_d, or growth, δ_g, distance vs. the wave frequency, f. ($n = 1-5\times10^9$ cm^{-3}, $B = 2000$ gauss). The bias on the metal tube is -30 volt.

the tube was -30 V and the confining magnetic field was 2000 Gauss. The e-folding length for the resulting axial density was ~ 12 cm. At any frequency, f, the corresponding wavelength is indicated by a cross. Above $f \sim 2$ kHz the waves are damped as they propagate away from the grid, and δ_d (triangles pointing upwards) is the damping distance. Below $f \sim 2$ kHz the relative amplitude of the waves increases with distance from the grid, and δ_g (triangles pointing downwards) is the growth distance. For $f \sim 2$ kHz we find $\delta \to \infty$ corresponding to undamped oscillations. We note from Figure 2:

a) $f\lambda$ = const $\approx 1.2\times10^5$ cm/s, as expected for the phase velocity of ion acoustic perturbations in this plasma,

b) for $f \gtrsim 3$ kHz, the ratio $\delta_d/\lambda \simeq 0.5$, independent of frequency: a well known feature of Landau damped ion acoustic waves, when $T_i \cong T_e$,

c) for $f \lesssim 1$ kHz, the growth distance δ_g is independent of frequency as predicted by both a hydrodynamic [9] and a microscopic theory [1, 2] for the case of gravitationally held atmosphere.

In order to fortify the results in Fig. 2, we show in Figs. 3 and 4 those obtained in somewhat different

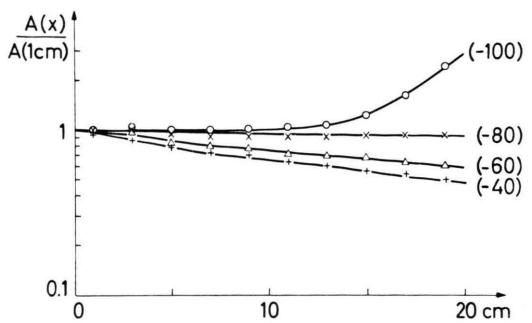

Fig. 3. Relative wave amplitude vs. axial distance for a fixed wave frequency, $f=1.5$ kHz. Each curve refers to a different bias on the metal tube, the bias in volt being shown in brackets ($B=3000$ gauss).

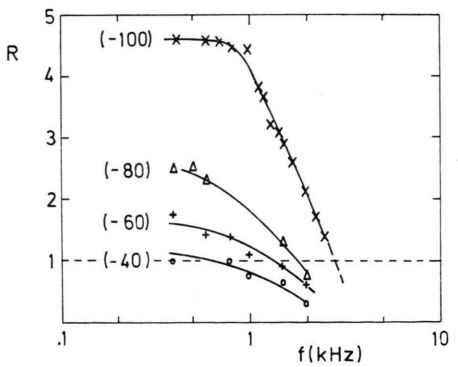

Fig. 4. The ration, R, of wave amplitude at $x_2=19$ cm from the grid to the wave amplitude at $x_1=5$ cm, vs. the wave frequency. In bracket is the tube bias in volt ($n=1-5\times10^9$ cm^{-3}, $B=3000$ gauss).

experiments. Figure 3 shows amplitude measurements as a function of x for a fixed frequency. The numbers in brackets indicate the bias of the metal tube (in volt). The transition between damping and relative growth is clearly demonstrated. Figure 4 shows the ratio, R, between the wave amplitude at a distance $x_2=19$ cm from the exciting grid and the wave amplitude at $x_1=5$ cm, plotted vs. frequency. The numbers in brackets indicate the tube bias in volts (more negative bias corresponding to a steeper axial density gradient). Clearly, as expected, the transition between growth and damping ($R=1$) moves to lower frequencies as the steepness of the density profile is reduced.

Finally, in Fig. 5, by utilizing data from the measurements of Fig. 2 and Fig. 4, we show the

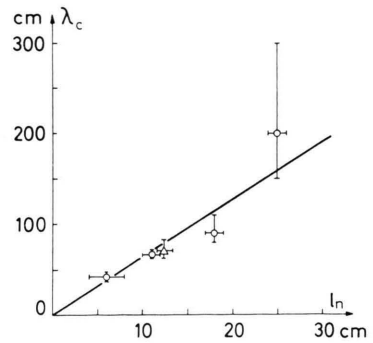

Fig. 5. The "critical" wavelength, λ_c, vs. the e-folding length of the axial density profile, l_n. The circles refer to the set of data in Fig. 4, the triangle to the data in Figure 2. The full line is the $\lambda_c=2\pi l_n$ line.

observed relation between the e-folding length, l_n, for the density and the critical wavelength, λ_c. The full line represents the relation $\lambda_c=2\pi l_n$.

In all the above measurements we assured ourselves that no wave reflection from the open end of the plasma column occurred. This point was checked by a) the actual wave phase measurements which showed that we were indeed dealing with propagating waves and b) by altering the boundary conditions of the "open" end (the one opposite to the hot plate), without affecting the observed wave behaviour.

It may be appropriate to mention here that nonlinearities were not observed in the above measurements. At extremely negative tube voltages ($V_{\text{tube}} \lesssim -100$ volt), however, pronounced harmonic generation was observed when a wave growing in relative amplitude was propagated. Typical results are shown in Figure 6. We explain this effect as follows. For these tube voltages radial losses are so strong that the unperturbed density on axis goes to zero within the tube (no plasma reaches the end plate). When $\tilde{n}/n_0 \sim 100\%$ the density gradient will have a rectifier (or "diode") effect (the total density cannot become negative), distorting the wave form and thus producing the harmonics. The wave form observed on an oscilloscope indeed showed a marked

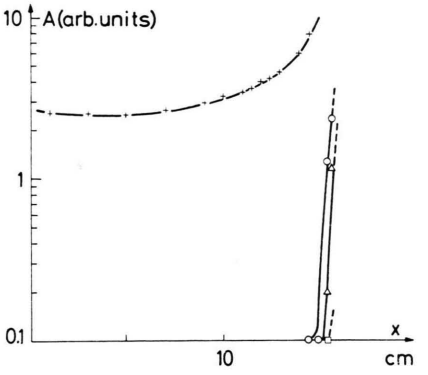

Fig. 6. Wave amplitude, at $f=1$ kHz, vs. axial distance, for $B=3000$ gauss and $V_{\text{tube}}=-150$ volt. At $x\gtrsim 14$ cm higher harmonics appear and grow (0, first harmonic; Δ, second harmonic; □, third harmonic).

flattening of the wave trough, thus supporting this interpretation. It is also interesting to note that, from measurements of the same type as for Fig. 1, we observe a very pronounced increase of $V_0(x)$ toward the "open" end of the colum, when $V_{\text{tube}} \lesssim -100$ volt.

IV. Theory

As mentioned in the introduction the theoretical results for a gravitationally held atmosphere (Refs. [1, 2, 9]) do not apply directly to our experimental conditions. In the following we give a simplified fluid theory directly related to our experimental set-up, which takes into account a) the radial losses and b) the non-zero drift velocity. A fluid theory cannot substitute a correct microscopic analysis. It remains, however, essentially correct in describing the zero-order state and the wave phenomena at very long wavelengths [10, 11]. The wavelength regime with $\lambda \ll l_n$ is, on the other hand, correctly described by the usual Vlasov-Landau treatment for a homogeneous plasma.

Starting from the equations

$$\frac{\partial n}{\partial t}+\frac{\partial}{\partial x}(n V)=-\gamma n\,, \tag{3}$$

$$n m\frac{\partial V}{\partial t}+n m V\frac{\partial V}{\partial x}+\varkappa(T_i+T_e)\frac{\partial n}{\partial x}=0\,, \tag{4}$$

we obtain the linear equations

$$\frac{\partial \zeta}{\partial t}+\frac{\partial v}{\partial x}-\frac{\gamma V_0}{V_0^2-C_s^2}v+V_0\frac{\partial \zeta}{\partial x}=0\,, \tag{5}$$

$$\frac{\partial v}{\partial t}+V_0\frac{\partial v}{\partial x}+\frac{C_s^2\gamma}{V_0^2-C_s^2}v+C_s^2\frac{\partial \zeta}{\partial x}=0 \tag{6}$$

where $\zeta=n/n_0$ and $C_s^2=\varkappa(T_i+T_e)/m$. The term $-\gamma n$ with $\gamma=$ const accounts for the radial losses according to the discussion in Section II. To solve the Eqs. (5) – (6) we assume $V_0\sim$ const. In view of Fig. 1 b this seems to be the best simplifying assumption. As already noted $V_0>C_s$ varies more slowly than n_0 and we are concerned with a solution for $\zeta=n/n_0(x)$. On the strength of this assumption we may apply elementary Fourier analysis and obtain

$$(\omega-k_r V_0)^2-k_i V_0^2-(k_r^2-k_i^2)C_s^2+\frac{k_i V_0\gamma C_s^2}{V_0^2-C_s^2}=0\,, \tag{7}$$

$$2k_i V_0(\omega-k_r V_0)+2k_r k_i C_s^2+\frac{k_r V_0\gamma C_s^2}{V_0^2-C_s^2}=0 \tag{8}$$

where k_r and k_i are the real and imaginary part of k, respectively, and ω is real corresponding to a boundary excitation. Using the zero order solution to (3)

$$n_0(x)=\frac{\text{const}}{V_0(x)}\exp\left\{-\gamma\int_0^x\frac{dx'}{V_0(x')}\right\} \tag{9}$$

we find $\gamma\cong V_0/l_n$ with the assumption of $V_0\sim$ const. Introducing this quantity in Eqs. (7) and (8) we obtain a numerical solution $\omega=\omega(k_r l_n)$ and $k_i=k_i(k_r)$, using the measured value of l_n. The calculations show that in the frequency range of interest k_i and ω/k_r are nearly constant, with $\omega/k_r\cong V_0+C_s$. If V_0 is determined from the measurements by using this relation, we find $V_0\cong 1.5\,C_s$ and with this value for V_0 we obtain $k_i l_n\cong 0.3$ or $\delta_g\cong 3\,l_n$, in good agreement with the results shown in Figure 2. (A cut-off frequency such as the one found in Ref. [3] does not appear in our calculations.) Near the damping-growth transition frequency these calculations do not hold.

For short wavelengths, as already remarked, the presence of the density gradient is unimportant and we expect the conventional Landau damping to be the dominant feature (see Section III).

A simple way of estimating the value of the transition wavelength, λ_c, is by noting that the growth-damping transition should occur at that wavelength for which the growth distance, δ_g (computed from fluid theory), equals the damping distance, δ_d (computed from the Vlasov-Landau theory for a uniform plasma). Since $\delta_d\cong 0.5\,\lambda$ and $\delta_g\cong 3\,l_n$, one obtains $\lambda_c\sim 6\,l_n$ (see Figure 5). It is also clear that

this simple argument applies to all cases in which there is competition between hydrodynamic growth and Landau damping, i.e. not only to the special case of a gravitationally hold atmosphere [1].

V. Conclusions

In this report we have presented measurements of ion acoustic wave propagation in a density gradient. The most interesting observation is that of a growth-damping transition at a critical wavelength, $\lambda_c \approx 2\pi l_n$. This result is in agreement with calculations performed on wave propagation in an isothermal atmosphere held by gravity [1, 2]. It thus appears that these calculations have a more general validity, i.e. they may apply independently of the particular way in which the density gradient is produced.

The relevance of the questions investigated in this report to the problem of the heating of the corona of the sun has already been noted [9]. Applications to problems where plasma expands from a finite region in space (e.g. laser produced plasmas) can be foreseen. As pointed out in Ref. [3] a similar experimental set-up may be convenient for generation of nonlinear ion waves of arbitray amplitude in a controlled manner. In order to see marked nonlinear effects our measurements show that the electron ion temperature ratio should be increased considerably (indeed in the experiment of Ref. [3] $T_e/T_i \gg 1$).

Acknowledgement

We thank M. Nielsen and B. Reher for their skilful technical assistance.

[1] D. Parkinson and K. Schindler, J. Plasma Phys. **3**, 13 [1969].
[2] C. H. Liu, J. Plasma Phys. **4**, 617 [1970].
[3] H. J. Doucet, W. D. Jones, and I. Alexeff, Phys. Fluids **17**, 1738 [1974].
[4] N. Rynn and N. D'Angelo, Rev. Sci. Instrum. **31**, 1326 [1960].
[5] N. D'Angelo, P. Michelsen, and H. L. Pécseli, Phys. Rev. Letters **34**, 1214 [1975].
[6] C. W. Roberson, A. S. Ratner, and J. L. Hirshfield, Phys. Rev. Letters **31**, 1041 [1973].
[7] A. Y. Wong, R. W. Motley, and N. D'Angelo, Phys. Rev. **133**, A 436 [1964].
[8] F. F. Chen, Phys. Fluids **9**, 965 [1966].
[9] N. D'Angelo, Astrophys. J. **154**, 401 [1968].
[10] H. Weitzner, Phys. Fluids **7**, 476 [1964].
[11] R. L. Liboff, Phys. Fluids **5**, 963 [1962].